




Cite this: *RSC Adv.*, 2019, 9, 6363

Facile synthesis of highly conductive PEDOT:PSS *via* surfactant templates

Phimchanok Sakunpongpitorn,^a Katesara Phasuksom,^a Nophawan Paradee^b and Anuvat Sirivat *^a

Poly(3,4-ethylenedioxythiophene):poly(styrenesulfonate) (PEDOT:PSS) nanoparticles in powder form with high electrical conductivity were synthesized *via* chemical oxidative polymerization. In addition, the effects of EDOT : PSS weight ratio, EDOT : Na₂S₂O₈ mole ratio, and surfactant concentration and type, namely hexadecyltrimethylammonium bromide (CTAB), sodium dodecylsulfate (SDS), and polyoxyethylene octyl phenyl ether (Triton X-100) on the properties of PEDOT:PSS were investigated. For the effect of EDOT : PSS weight ratio, at the EDOT : Na₂S₂O₈ mole ratio of 1 : 1, the EDOT : PSS weight ratio of 1 : 11 was the optimal condition to obtain electrical conductivity of 999.74 ± 10.86 S cm⁻¹ due to the high amount of PSS⁻ and SO₄²⁻ available to interact with the PEDOT chain with a low % PSSNa. For the effect of EDOT : Na₂S₂O₈ mole ratio, at the EDOT : PSS weight ratio of 1 : 11, the EDOT : Na₂S₂O₈ mole ratio of 1 : 2 was the best condition as it provided the highest dopant (PSS⁻ and SO₄²⁻) amount, while the % PSSNa was relatively low. For the effect of surfactant type and concentration, at the EDOT : PSS weight ratio of 1 : 11 and EDOT : Na₂S₂O₈ mole ratio of 1 : 2, Triton X-100 at 2.5CMC provided electrical conductivity higher than with CTAB and SDS. The thermal stability of PEDOT:PSS obtained from various conditions was investigated, and PEDOT:PSS without surfactant showed the highest thermal stability since it produced the highest char yield. In this study, the highest electrical conductivity of PEDOT:PSS, which was obtained in the presence of Triton X-100 to reduce the PSSNa amount, was 1879.49 ± 13.87 S cm⁻¹, the highest value reported to date.

Received 24th October 2018
 Accepted 6th February 2019

DOI: 10.1039/c8ra08801b

rsc.li/rsc-advances

1. Introduction

Conductive polymers (CPs) are organic polymers that are different from typical polymers because they can conduct electricity through their conjugated structures, consisting of alternating double (π) bonds and single (σ) bonds along the CP chains.¹ CPs have sp² hybridization in their backbones, in which the p-orbital in each atom is perpendicular to the plane of the polymer chain but parallel to each other, allowing electron delocalization along the polymer chains.² The first conductive polyacetylene was discovered in 1977,³ and since then, many CPs have been intensively investigated. Some common and interesting CPs include polypyrrole (PPy), polyaniline (PANI), polythiophene (PT), *trans*-polyacetylene, poly(*p*-phenylene vinylene), and poly(3,4-ethylenedioxythiophene) (PEDOT).⁴ CPs have many advantageous properties such as chemical diversity, low density, flexibility, corrosion resistance, controllable morphology, and tunable conductivity.^{5,6} Therefore, CPs are utilized in many applications, such as polymer light-emitting diodes,⁷ organic

transistors,⁸ actuators,⁹ anti-static coatings, sensors, batteries, solar cells,¹⁰ and drug delivery.¹¹

Poly(3,4-ethylenedioxythiophene) (PEDOT) is one of most studied conductive polymers owing to its relatively high electrical conductivity and electro-optical properties. PEDOT can be synthesized *via* both chemical oxidative polymerization and electrochemical polymerization. However, chemical oxidative polymerization provides a higher yield with no special setup required.¹² Although PEDOT has high electrical conductivity, it is insoluble in water, making it difficult to process. This problem is overcome by using a polyelectrolyte, poly(styrenesulfonic acid) (PSS), which acts as a dopant and stabilizer for PEDOT through charge balance.¹³

Poly(3,4-ethylenedioxythiophene):poly(styrenesulfonate) (PEDOT:PSS) is a PEDOT derivative, which has higher electrical conductivity as compared to other CPs.¹⁴ Moreover, it has other useful properties, such as high transparency,¹⁵ low thermal conductivity, low density, good flexibility, and high thermal stability.¹⁶ In general, PEDOT:PSS is used in various electrical and optical devices, such as thin film transistors, light-emitting diodes, sensors, and photovoltaics.¹⁷

The electrical conductivity of PEDOT:PSS can be enhanced by solvent treatment,¹⁸ adding surfactant,¹⁹ and varying the PSS concentration.²⁰ Ouyang *et al.* investigated the effect of organic

^aThe Conductive and Electroactive Polymers Research Unit, The Petroleum and Petrochemical College, Chulalongkorn University, Bangkok 10330, Thailand. E-mail: anuvat.s@chula.ac.th

^bDepartment of Chemistry, Faculty of Science, King Mongkut's University of Technology Thonburi, Bangkok, 10140, Thailand



solvent treatment using secondary dopants, such as acetonitrile (ACN), 4-methoxyphenol, *N,N*-dimethylacetamide (DMAc), *N*-methyl-2-pyrrolidone (NMP), ethylene glycol (EG), and dimethyl sulfoxide (DMSO) to increase the electrical conductivity of the PEDOT:PSS film. The highest electrical conductivity of a PEDOT:PSS film treated with DMSO was 200 S cm^{-1} .¹⁸ Oh *et al.* studied the effect of Triton X-100 (nonionic surfactant) on the electrical conductivity of PEDOT:PSS films, which increased from 0.85 ± 0.08 to $882 \pm 75 \text{ S cm}^{-1}$ at a Triton X-100 concentration of 1.0 wt%.¹⁹ Horri *et al.* studied the effect of EDOT : PSS weight ratio on the electrical conductivity of PEDOT:PSS films, and an EDOT : PSS weight ratio of 1 : 2.3 provided the highest electrical conductivity of 700 S cm^{-1} .²⁰

Alternatively, PEDOT:PSS can be prepared in powder form, which can be subsequently modified and processed for various applications, such as proton exchange membrane fuel cells,²¹ actuators,²² and sensors.²³ Lefebvre *et al.* studied the effect of the PEDOT:PSS weight ratio in the range of 1 : 2.5 to 1 : 7.5, where the electrical conductivity of the PEDOT:PSS powder varied from 0.3 to 1.3 S cm^{-1} .²⁴ Wichaianssee *et al.* synthesized PEDOT:PSS powder *via* chemical oxidative polymerization at room temperature using sodium persulfate ($\text{Na}_2\text{S}_2\text{O}_8$) as the oxidizing agent and ferric sulphate ($\text{Fe}_2(\text{SO}_4)_3$) as the catalyst. The synthesized PEDOT:PSS powder possessed electrical conductivity of $27.5 \pm 0.6 \text{ S cm}^{-1}$.²² Chanthanont *et al.* synthesized PEDOT:PSS powder using $\text{Na}_2\text{S}_2\text{O}_8$ as the oxidizing agent and $\text{Fe}_2(\text{SO}_4)_3$ as the catalyst in aqueous solution at room temperature, and the electrical conductivity of the PEDOT:PSS powder was determined to be $11.69 \pm 0.006 \text{ S cm}^{-1}$.²³ In summary, it can be noted that PEDOT:PSS in the powder form has relatively lower electrical conductivity than that of its films, as previously reported.

Herein, we report the synthesis of PEDOT:PSS nanoparticles with high electrical conductivity *via* chemical oxidative polymerization in aqueous solution at room temperature. The effects of the EDOT : PSS weight ratio, EDOT : $\text{Na}_2\text{S}_2\text{O}_8$ mole ratio, and surfactant type and concentration on the properties of PEDOT:PSS were systematically investigated. The PEDOT:PSS powder samples were characterized *via* Fourier transform infrared spectroscopy (FT-IR), Raman spectroscopy (Raman), and wide-angle X-ray spectroscopy (XRD) to determine their chemical structure, X-ray photoelectron spectroscopy (XPS) to analyze their element contents, UV-Vis spectrophotometry (UV-Vis) to determine their doping state, and field-emission scanning electron microscopy (FE-SEM) to determine their particle shape and size. Thermogravimetric analysis (TG-DTA) was used to determine their thermal stability. It was found that the PEDOT:PSS powder with the EDOT : PSS weight ratio of 1 : 11, EDOT : $\text{Na}_2\text{S}_2\text{O}_8$ mole ratio of 1 : 2, and Triton X-100 at the concentration of 2.5CMC possessed the highest electrical conductivity of $1879.49 \pm 13.87 \text{ S cm}^{-1}$ with the corresponding spherical particle size of $56.77 \pm 5.54 \text{ nm}$, values not previously obtained to date.

2. Experimental

2.1 Materials

3,4-Ethylenedioxythiophene (EDOT, 97% purity) monomer, poly(styrenesulfonate) (PSS, 99% purity) with M_w of 75 000 g

mol^{-1} , hexadecyltrimethylammonium bromide (CTAB, $\geq 96\%$ purity), and sodium persulfate ($\text{Na}_2\text{S}_2\text{O}_8$, $\geq 98\%$ purity) were purchased from Sigma Aldrich. Sodium dodecylsulfate (SDS, $\geq 99\%$ purity) and polyoxyethylene octyl phenyl ether (Triton X-100, $\geq 99\%$ purity) were purchased from Omnipur. Methanol ($>99.8\%$ purity) and acetone (99.5% purity) were purchased from RCI Labscan. Distilled water was used as the solvent in the synthesis. All reagents were of analytical reagent grade.

2.2 Synthesis of PEDOT:PSS

To investigate the effect of the EDOT : PSS weight ratio, 0.5 g of EDOT was mixed with PSS ranging from 0.5 g to 6.5 g (weight ratios of 1–13), where the $\text{Na}_2\text{S}_2\text{O}_8$ content as the oxidant was fixed at 0.8335 g to give the EDOT : $\text{Na}_2\text{S}_2\text{O}_8$ mole ratio of 1 : 1. The ingredients were dissolved in 100 mL of DI water, then the solution was stirred for 24 h at room temperature. The precipitate was collected by centrifugation at 9000 rpm, rinsed with a mixed solution of acetone : methanol with a volume ratio of 3 : 20,²⁵ and then dried in an oven at $60 \text{ }^\circ\text{C}$ for 24 h.

To determine the effect of the EDOT : $\text{Na}_2\text{S}_2\text{O}_8$ mole ratio, the synthesis procedure was the same as before. 0.83, 1.25, 1.67, 2.08, 2.50, and 3.33 g of $\text{Na}_2\text{S}_2\text{O}_8$ were added to 0.5 g of EDOT to give the EDOT : $\text{Na}_2\text{S}_2\text{O}_8$ mole ratios of 1 : 1, 1 : 1.5, 1 : 2, 1 : 2.5, 1 : 3, 1 : 4, and the EDOT : PSS weight ratio was fixed at 1 : 11 (0.5 g : 5.5 g).

To study the effect of surfactant type, namely CTAB, SDS, and Triton X-100, and concentration, each surfactant (0.084 g, 0.721 g, 0.141 g, respectively) was added to 100 mL of distilled water and stirred for 1 h to form a surfactant solution at 2.5CMC. Then 0.5 g of EDOT was added in the surfactant solution, which was continuously stirred for 1 h. Then PSS (5.5 g) was added to the above solution, and it was stirred for 1 h before the $\text{Na}_2\text{S}_2\text{O}_8$ oxidant (1.67 g) was added. The EDOT : PSS weight ratio was fixed at 1 : 11 and the EDOT : $\text{Na}_2\text{S}_2\text{O}_8$ mole ratio was 1 : 2. The solution was stirred continuously for 24 h at room temperature, and the color of the solution changed from clear to dark blue. The precipitate was centrifuged at 9000 rpm and then washed with a solution of acetone : methanol at the volume ratio of 3 : 20. Finally, the precipitate was dried in an oven at $60 \text{ }^\circ\text{C}$ for 24 h. Next, the PEDOT:PSS precipitate was ground in a mortar by hand for 3 min to obtain the PEDOT:PSS powder with smaller particle sizes, which was further modified for characterization.²⁶ Lislie *et al.* reported that grinding PPy with a mortar and pestle for 10 min did not significantly change its electrical conductivity.²⁶ However, Fufang *et al.* reported that the electrical conductivity of PPy decreased by 21% and the particle size decreased by 26% after grinding in a mortar for 1 h.²⁷

2.3 Characterization of PEDOT:PSS nanoparticles

The critical micelle concentration (CMC) of PSS was determined by measuring its surface tension using a tensiometer (Kruss/Easydyne tensiometer, K20) with the Wilhelmy plate mode at $23 \text{ }^\circ\text{C}$. PSS was dissolved in deionized water at various EDOT : PSS weight ratios. The CMC of PSS was found to be $7 \times 10^{-5} \text{ mol L}^{-1}$.



The functional group analysis was carried out *via* Fourier transformed infrared spectroscopy, FTIR (Thermo Nicolet, Nexus 670). All spectra were recorded in the wavenumber range of 400–4000 cm^{-1} , with 32 scans and a resolution of 4 cm^{-1} . The PEDOT:PSS samples were mixed with background KBr powder and compressed using a hydraulic press machine.

The chemical and structural information of the PEDOT:PSS powder were identified *via* Raman spectroscopy (Bruker, Ram II) with a laser source at 1064 nm and power of 22 mW. All spectra were recorded in the wavenumber range of 400–4000 cm^{-1} , with 800 scans and a resolution of 4 cm^{-1} .

The PEDOT:PSS crystalline structure was identified *via* wide-angle X-ray spectroscopy, XRD (Rigaku/Smartlab), at a scan step of 0.02° and scan speed of 5° min^{-1} in the 2θ range of 5° to 70°. The Cu-K α radiation source was operated at 40 kV/30 mA. The PDLX 2 software was used to analyze the PEDOT:PSS XRD patterns.

The element analysis was carried out *via* X-ray photoelectron spectroscopy, XPS (Kratos, Axis Ultra DLD), using a monochromatized Al K α radiation source and recorded at the analyzer pass energy of 160 eV for the survey scan, and at 40 eV for the high-resolution scan. All spectra were corrected by using the reference C 1s (binding energy of 284.8 eV). The Casa-XPS software was used for the interpretation of the XPS spectra.

The doping state and optical band gap of PEDOT:PSS was identified *via* UV-Vis spectrophotometry, UV-Vis (Tecan, The Infinite® 200 PRO NanoQuant). The PEDOT:PSS powders were dissolved in deionized water and filtered using a nylon filter. Deionized water was used as the reference. The i-Control software was used to determine the UV adsorption of the PEDOT:PSS solutions. The band gap energy was calculated using the Tauc eqn (1):²⁸

$$\alpha hv = A(hv - E_g)^n \quad (1)$$

where α is the adsorption coefficient, $h\nu$ is the photon energy (eV), h is Planck's constant, ν is the frequency (s^{-1}), A is a constant, E_g is the band gap energy (eV), and n is equal to 0.5 for direct transitions. The adsorption coefficient (α) was calculated from the Beer–Lambert's relation (2):²⁹

$$\alpha = 2.303Ab/I \quad (2)$$

where, Ab is the absorbance and I is the sample path length. The extrapolation of the linear line from the plot between $(\alpha h\nu)^2$ on the y axis and $h\nu$ on the x axis gives E_g .

The morphology of PEDOT:PSS was identified *via* field-emission scanning electron microscopy, FE-SEM (Hitachi, S-4800), operating at 5 kV/10 μA at a magnification of 100 000. Each sample was distributed on the sample holder with a carbon adhesive tape and coated with a thin layer of platinum before the measurement.

The thermal analysis was carried out using a thermogravimetric analyzer, TG-DTA (Perkin Elmer, TGA model 7). 4 to 8 mg of each sample was loaded into an aluminum pan. The sample was scanned from 30 °C to 800 °C at a heating rate of 10 °C min^{-1} under a nitrogen flow.

The electrical conductivity was measured using an electrometer (Keithley, model 17A) at room temperature in air. A custom-built two-point probe was used as a fixture for each PEDOT:PSS pellet. The graph between I (y -axis) and V (x -axis) was plotted to obtain the I - V slope, which was used to calculate the electrical conductivity according to eqn (3):³⁰

$$\sigma = I/KVt = (I-V) \text{ slope}/Kt \quad (3)$$

where, I is the current (A), V is the applied voltage (V), t is the sample thickness (cm), and K is the correction factor calculated using a silicon wafer as the reference. PEDOT:PSS pellets with 0.7 ± 0.3 mm thickness and 1.3 cm diameter were prepared by compressing the PEDOT:PSS powder with a hydraulic press machine.

3. Results and discussion

The PEDOT:PSS powder was synthesized *via* chemical oxidative polymerization following the procedure shown in Scheme 1. In the initial step, $\text{Na}_2\text{S}_2\text{O}_8$ as the oxidant dissociates into sodium ions and a persulfate ion, where the persulfate ion can homolytically dissociate into sulfate radicals in aqueous solution, as shown in Scheme 1(a).³¹ In the oxidation step, an EDOT monomer is oxidized to an EDOT radical cation by the sulfate radical, leading to the formation of sulfate anions, as shown in Scheme 1(b).³² For the propagation and doping step, the coupling of EDOT radical cations generates two protons, which are removed in this step. Simultaneously, the PSS and sulfate ions acting as dopants can interact with the oxidized PEDOT chains during the polymerization. The sodium ion from the oxidant can also react with the PSS chains, as illustrated in Scheme 1(c).

3.1 Structural conformation of PEDOT:PSS

3.1.1 FTIR analysis. The functional groups of PEDOT:PSS synthesized under various conditions were characterized *via* FTIR, as shown in Fig. 1. The FTIR spectrum of PEDOT:PSS (Fig. 1(a)), at the EDOT : PSS weight ratio of 1 : 11 and EDOT : $\text{Na}_2\text{S}_2\text{O}_8$ mole ratio of 1 : 2 shows peaks at 1640 and 1518 cm^{-1} , which are assigned to the C=C stretching in the aromatic rings of PSS³³ and the C=C stretching in the thiophene ring of PEDOT,³⁴ respectively. The peak at 1340 cm^{-1} indicates the C–C stretching from the thiophene ring of PEDOT.³⁴ The symmetric stretching and antisymmetric stretching of S=O can be seen at 1198 and 1055 cm^{-1} , respectively, belonging to PSS and SO_4^{2-} from the oxidant.³⁴ The peaks at 1145 and 983 cm^{-1} can be attributed to the S–O stretching in PSS and SO_4^{2-} from the oxidant and the S–phenyl bond in PSS, respectively.³⁵ The three peaks at 936, 840, and 691 cm^{-1} correspond to the C–S stretching of the thiophene ring in PEDOT.³⁵ The two peaks at 1144 and 1092 cm^{-1} are correspond to the C–O stretching of PEDOT.²³ The peaks at 3415, and 2921 cm^{-1} correspond to the O–H stretching of PSS and C–H stretching of PEDOT and PSS, respectively, resulting from PSS incorporated in the PEDOT chain.³⁴ For the PEDOT:PSS synthesized without surfactant at various





Scheme 1 Proposed mechanism for the oxidative polymerization of PEDOT:PSS.



Fig. 1 FTIR spectra of PEDOT:PSS at the EDOT : PSS weight ratio of 1 : 11 and EDOT : $\text{Na}_2\text{S}_2\text{O}_8$ mole ratio of 1 : 2 with various surfactant types: (a) no surfactant, (b) CTAB (2.5CMC), (c) SDS (2.5CMC), and (d) Triton X-100 (2.5CMC).

EDOT : PSS weight ratios and EDOT : $\text{Na}_2\text{S}_2\text{O}_8$ mole ratios, their FTIR spectra showed the same functional groups as that with the EDOT : PSS weight ratio of 1 : 11 and EDOT : $\text{Na}_2\text{S}_2\text{O}_8$ mole ratio of 1 : 2. The FTIR spectra of the synthesized PEDOT:PSS (Fig. 1(a)) are similar to the PEDOT:PSS spectrum reported by Chanthanont and Sirivat, 2013.²³

The FTIR spectrum of PEDOT:PSS synthesized in CTAB (Fig. 1(b)) shows peaks at 2973 and 2898 cm^{-1} , indicating the $\text{CH}_3\text{-N}^+$ anti-symmetric stretching and C-H stretching, respectively, which confirm the incorporation of CTAB in PEDOT:PSS.³⁶ In the case of PEDOT:PSS prepared with SDS (Fig. 1(c)), the O-H stretching peak shifts from 3415 to 3339 cm^{-1} because SDS can repel the O-H of PSS by electro-repulsive forces.³⁷ For the system of Triton X-100, the FTIR spectrum of PEDOT:PSS (Fig. 1(d)) is the same as that without surfactant, and it does not show any characteristic peaks of Triton X-100. Thus, Triton X-100 was not incorporated in PEDOT:PSS.

For the PEDOT:PSS synthesized at various CTAB concentrations, at the EDOT : PSS weight ratio of 1 : 11 and



EDOT : Na₂S₂O₈ mole ratio of 1 : 2, the spectra show the CH₃-N⁺ anti-symmetric stretching of CTAB at 2973 cm⁻¹ and the C-H stretching peak at 2898 cm⁻¹,³⁶ where the intensity of the former increased with an increase in CTAB concentration. In the case of various SDS concentrations, the intensity of the O-H stretching peak of SDS located at 3339 cm⁻¹ (ref. 38) increased with an increase in SDS concentration. Under various Triton X-100 concentrations, the FT-IR spectra of PEDOT:PSS were nearly the same with an increase in Triton X-100 concentration.

3.1.2 FT Raman analysis. The PEDOT:PSS synthesized at the EDOT : PSS weight ratios of 1 : 5, 1 : 11, and 1 : 13 and EDOT : Na₂S₂O₈ mole ratio fixed at 1 : 1 were characterized using the FT Raman technique. The FT Raman spectra showed the dominant peak at 1424 cm⁻¹, indicative of the C_α-C_β stretching vibration mode of the quinoid structure in PEDOT.³⁹ The quinoid structure represents the linear structure or the expanded-coil of the PEDOT:PSS chain, which lies on the same plane. Hence, the conjugated π-electrons can delocalize in the PEDOT chain.⁴⁰ The PEDOT:PSS synthesized at the EDOT : PSS weight ratio of 1 : 11 and EDOT : Na₂S₂O₈ mole ratio of 1 : 2 with Triton-X 100 (2.5CMC) was also characterized *via* FT-Raman spectroscopy and it was observed that the FT-Raman spectrum with the surfactant was similar to that without surfactant, indicating the same quinoid structure in the PEDOT chain.

3.2 X-ray diffraction

The XRD patterns of PEDOT:PSS with different EDOT : PSS weight ratios at the EDOT : Na₂S₂O₈ mole ratio of 1 : 1 are shown in Fig. 2. The two main peaks at 2θ = 17.7° and 25.8° refer to the amorphous halo diffraction of PSS and the inter-chain packing of PEDOT, respectively.⁴¹ At the EDOT : PSS weight ratios ranging from 1 : 9 to 1 : 11, the peaks in the XRD patterns show a shift from 25.5° to 25.8°, which is consistent with the smaller *d*-spacings between the PEDOT chains ranging from 3.48 Å to 3.45 Å. However, the intensities of the crystalline peaks of EDOT : PSS at the weight ratio of 1 : 11 were lower than that of the other EDOT : PSS weight ratios, suggesting that the PEDOT:PSS at this condition possessed a lower PSSNa content. PSSNa is a salt that reduces the available doping sites on PSS, and hence induces charge screening between PEDOT and PSS.⁴² Zotti *et al.*, 2003, reported that the electrical conductivity of PEDOT:PSS was reduced due the presence of PSSNa in PEDOT:PSS.⁴³

Fig. 3 illustrates the XRD patterns of commercial PSSNa and PEDOT:PSS synthesized using various EDOT : Na₂S₂O₈ mole ratios at the EDOT : PSS weight ratio of 1 : 11. The PSSNa XRD pattern showed crystalline peaks at 19.1°, 23.2°, 28.1°, 29.1°, 32.2°, 34.0°, 38.7° and 48.9°.⁴⁴ The two main peaks of PEDOT:PSS are evident at 2θ = 17.7° and 2θ = 25.8°, similar to the results in Fig. 2. However, the intensities of the crystalline peak of PSSNa incorporated in PEDOT:PSS tended to increase with an increase in EDOT : Na₂S₂O₈ mole ratio because sodium ions from the oxidant are more prone to interact with PSS molecules by electrostatic interaction.⁴⁴ The increase in PSSNa with an increase in EDOT : Na₂S₂O₈ mole ratio was further investigated by XPS.

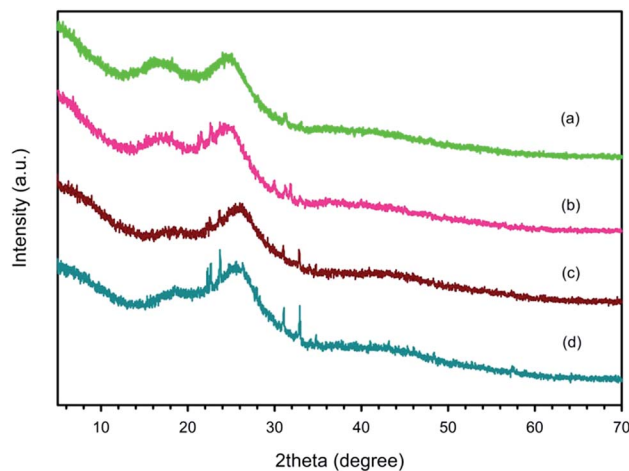


Fig. 2 XRD spectra of PEDOT:PSS at the EDOT : Na₂S₂O₈ mole ratio of 1 : 1 and at various EDOT : PSS weight ratios: (a) EDOT : PSS weight ratio of 1 : 1, (b) EDOT : PSS weight ratio of 1 : 5, (c) EDOT : PSS weight ratio of 1 : 11, and (d) EDOT : PSS weight ratio of 1 : 13.

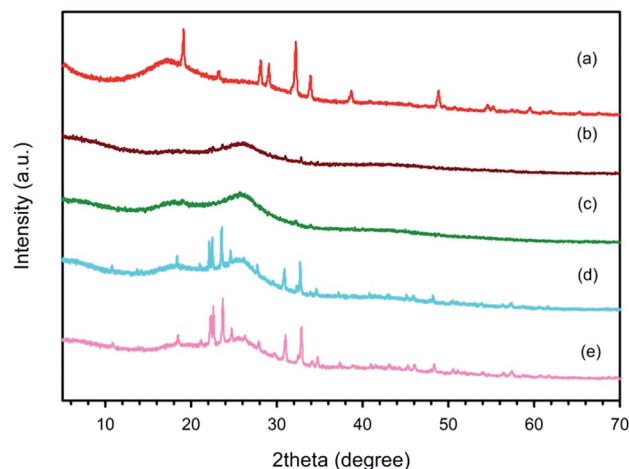


Fig. 3 XRD spectra of commercial PSSNa and PEDOT:PSS at the EDOT : PSS weight ratio of 1 : 11 and at various EDOT : Na₂S₂O₈ mole ratios: (a) PSSNa, and EDOT : Na₂S₂O₈ mole ratio of (b) 1 : 1, (c) 1 : 2, (d) 1 : 3 and (e) 1 : 4.

The PEDOT:PSS synthesized using various surfactant types and concentrations at the EDOT : PSS weight ratio of 1 : 11 and EDOT : Na₂S₂O₈ mole ratio of 1 : 2 were also investigated *via* XRD. The obtained XRD patterns were nearly the same as that without surfactant, suggesting the surfactants did not affect the crystallinity of PEDOT:PSS.

3.3 X-ray photoelectron spectroscopy

The element analysis and chemical bonding of the synthesized PEDOT:PSS were characterized by XPS. The wide-scan XPS spectra of PEDOT:PSS revealed the peaks of Na 1s, O 1s, C 1s, and S 2p located at 1066.0, 527.0, 280.0, and 163.0 eV, respectively. The existence of Na in PSSNa⁴⁴ is due to the interaction of PSS⁻ and Na⁺ from the oxidant. The high-resolution scan XPS



Table 1 XPS deconvoluted contribution of S (sulphur) 2p of PEDOT:PSS synthesized at various conditions

Sample code	% PEDOT	% PSS ⁻ and % SO ₄ ²⁻	% PSSNa
Effect of PSS (no surfactant)			
Pure PEDOT (without PSS)	85.41	14.59	—
EDOT : PSS weight ratio of 1 : 1 and EDOT : Na ₂ S ₂ O ₈ mole ratio of 1 : 1	62.96	21.23	15.89
EDOT : PSS weight ratio of 1 : 11 and EDOT : Na ₂ S ₂ O ₈ mole ratio of 1 : 1	31.47	45.57	22.96
EDOT : PSS weight ratio of 1 : 13 and EDOT : Na ₂ S ₂ O ₈ mole ratio of 1 : 1	36.43	39.89	23.68
Effect of oxidant (no surfactant)			
EDOT : PSS weight ratio of 1 : 11 and EDOT : Na ₂ S ₂ O ₈ mole ratio of 1 : 1	31.47	45.57	22.96
EDOT : PSS weight ratio of 1 : 11 and EDOT : Na ₂ S ₂ O ₈ mole ratio of 1 : 2	29.05	50.59	20.36
EDOT : PSS weight ratio of 1 : 11 and EDOT : Na ₂ S ₂ O ₈ mole ratio of 1 : 4	19.56	35.27	45.13
Effect of surfactant			
EDOT : PSS weight ratio of 1 : 11 and EDOT : Na ₂ S ₂ O ₈ mole ratio of 1 : 2 with Triton X-100 (at CMC)	27.80	49.78	22.42
EDOT : PSS weight ratio of 1 : 11 and EDOT : Na ₂ S ₂ O ₈ mole ratio of 1 : 2 with Triton X-100 (at 2.5CMC)	45.40	37.52	17.08
EDOT : PSS weight ratio of 1 : 11 and EDOT : Na ₂ S ₂ O ₈ mole ratio of 1 : 2 with Triton X-100 (at 5CMC)	42.53	37.42	20.05
EDOT : PSS weight ratio of 1 : 11 and EDOT : Na ₂ S ₂ O ₈ mole ratio of 1 : 2 with Triton X-100 (at 10CMC)	47.81	36.46	19.22
EDOT : PSS weight ratio of 1 : 11 and EDOT : Na ₂ S ₂ O ₈ mole ratio of 1 : 2 with CTAB (at 2.5CMC)	15.34	30.57	54.09
EDOT : PSS weight ratio of 1 : 11 and EDOT : Na ₂ S ₂ O ₈ mole ratio of 1 : 2 with SDS (at 2.5CMC)	45.82	34.32	19.87

spectra of S 2p showed the deconvolution of S 2p of PEDOT:PSS, which indicated the C-S of PEDOT was located at 163.22 and 164.46 eV,⁴⁵ S=O of SO₄²⁻ from the oxidant and S=O of SO₃⁻ from PSS at 168.21 and 169.10 eV,^{46,47} respectively, and S=O from PSSNa at 169.81 and 170.59 eV.^{48,49} The element and chemical bonding of PEDOT (without PSS) was also investigated *via* XPS for comparison with PEDOT:PSS. The wide-scan XPS spectrum of pure PEDOT showed the elements C 1s, O 1s, and S 2p without Na. Thus, it can be confirmed that PSS is the main component inducing the formation of PSSNa. The deconvolution of S 2p indicated the C-S of the pure PEDOT at 163.22 and 164.46 eV,⁵⁰ and S=O of SO₄²⁻ from the oxidant at 167.53 and 168.59 eV,⁴⁷ suggesting that SO₄²⁻ from the oxidant acts as a dopant by interacting with PEDOT through electrostatic interaction.¹² The S=O of PSSNa was not found in the S 2p deconvolution of the pure PEDOT (without PSS), while it was present for PEDOT:PSS. The atom percentages of the sulphur species from PEDOT, PSS⁻, SO₄²⁻ and PSSNa are tabulated in Table 1, where both PSS⁻ and SO₄²⁻ act as dopants for the oxidized PEDOT chain.

For the effect of EDOT : PSS weight ratios, at the EDOT : Na₂S₂O₈ mole ratio of 1 : 1, Table 1 shows that the % PSS⁻ and % SO₄²⁻ tended to increase with an increase in EDOT : PSS weight ratio because PSS⁻ acts as a dopant. However, at the EDOT : PSS weight ratio of 1 : 13, the decrease in % PSS⁻ and % SO₄²⁻ was due to the over-doping or excessive PSS.⁵¹ In the present work, the PEDOT:PSS synthesized at the EDOT : PSS weight ratio of 1 : 11 possessed the highest % PSS⁻ and % SO₄²⁻ compared to other EDOT : PSS weight ratios and with a low % PSSNa. Thus, the high amount of dopants (% PSS⁻ and % SO₄²⁻) is available to provide a high number of charge carriers.⁵² On the other hand, PSSNa reduces the number of doping sites on PSS, and thus induces charge screening between the PEDOT and PSS chains.⁴² Therefore, EDOT : PSS at the weight ratio of 1 : 11 is optimal for the synthesis of PEDOT:PSS.

For the effect of EDOT : Na₂S₂O₈ mole ratio, at the EDOT : PSS weight ratio of 1 : 11, the EDOT : Na₂S₂O₈ mole ratio of 1 : 2 possessed the highest % PSS⁻ and % SO₄²⁻ (50.59%), while the % PSSNa was relatively low (20.36%), as shown in Table 1. The increase in % PSS⁻ and % SO₄²⁻ is because the SO₄²⁻ ions from the oxidant prefer to interact with the PEDOT chain. However, at a higher EDOT : Na₂S₂O₈ mole ratio, the PSSNa content tends to increase as Na⁺ ions from the oxidant largely interact with PSS⁻ to form PSSNa.⁴⁴ This suggests that the PEDOT:PSS interaction is reduced by the existence of PSSNa *via* a reduction in doping sites and its screening. Thus, the EDOT : Na₂S₂O₈ mole ratio of 1 : 2 is optimal since it provided the highest dopant content (% PSS⁻ and % SO₄²⁻), while % PSSNa is relatively low.

For the effect of surfactant type, at the EDOT : PSS weight ratio of 1 : 11 and the EDOT : Na₂S₂O₈ mole ratio of 1 : 2, each surfactant differently affected the presence of sulphur species in PEDOT:PSS. The PEDOT:PSS synthesized with CTAB (2.5CMC) possessed a lower % PSS⁻ and % SO₄²⁻ than that with SDS and Triton X-100, respectively, as shown in Table 1. CTAB is a cationic surfactant, which can interact with PSS⁻ (negatively charged) *via* electrostatic interaction, and thus reduces the interaction between PEDOT and PSS.⁵³ For the SDS system (2.5CMC), SDS is an anionic surfactant, which prefers to interact with PEDOT instead of PSS⁻,³⁷ resulting in a higher % PEDOT than that without surfactant. For the Triton X-100 system (2.5CMC), the PEDOT:PSS possessed a higher % PSS⁻ and % SO₄²⁻ and a lower % PSSNa than that with the other two surfactants.

For effect of Triton X-100 concentration, as shown in Table 1, Triton X-100 forms micelles at its CMC,³⁰ but they are unstable. At high Triton X-100 concentrations of 2.5CMC, 5CMC and 10CMC, the % PSSNa was lower, while % PSS⁻ and % SO₄²⁻ decreased with an increase in concentration. Triton X-100 is a non-ionic surfactant that can interact with both PEDOT and PSS. However, the resulting TX-PSS complex can be easily



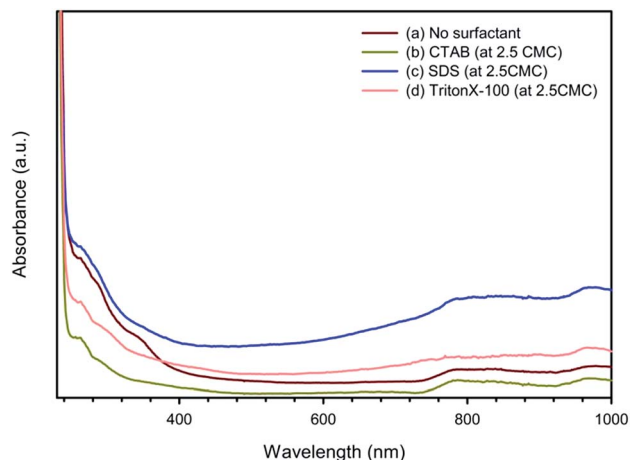


Fig. 4 UV adsorption spectra of PEDOT:PSS at the EDOT : PSS weight ratio of 1 : 11 and EDOT : Na₂S₂O₈ mole ratio of 1 : 2 using various surfactant types: (a) no surfactant, (b) CTAB (at 2.5CMC), (c) SDS (at 2.5CMC), and (d) Triton X-100 (at 2.5CMC).

removed by washing with methanol,⁵⁴ resulting in the simultaneous removal of PSS⁻ as a dopant and PSSNa as a salt. This suggests that Triton X-100 at higher concentrations than 2.5CMC reduces the PEDOT and PSS interaction as well as the PSSNa amount.

3.4 UV-visible spectroscopy

3.4.1 Characteristics of UV spectra. The UV adsorption spectra of PEDOT:PSS synthesized at the EDOT : PSS weight ratio of 1 : 11 and EDOT : Na₂S₂O₈ mole ratio of 1 : 2 with surfactants (at 2.5CMC) and without surfactant are shown in Fig. 4. All the UV spectra show a UV absorbance at 258 nm, which can be assigned to the substituted phenyl groups in PSS.⁵⁵ The broad bands between 600 and 900 nm and between 700 to 1000 nm can be ascribed to the polaron and bipolaron states of PEDOT:PSS, respectively, indicative of the characteristic doped state of PEDOT:PSS.²⁵

For the effects of EDOT : PSS weight ratio and EDOT : Na₂S₂O₈ mole ratio, the characteristics of the PEDOT:PSS UV-spectra were nearly the same with an increase in EDOT : PSS weight ratio or increase in EDOT : Na₂S₂O₈ mole ratio, consistent with previous work of Khan and Narula, 2016.²⁵

3.4.2 Band gap energy. The band gap energy of PEDOT:PSS was calculated by using the Tauc relation (eqn (1)), as tabulated in Table 2. In the case of various EDOT : PSS weight ratios, the band gap energy of PEDOT:PSS prepared at the EDOT : PSS weight ratio of 1 : 5 (2.92 eV) was higher than that for the EDOT : PSS weight ratio of 1 : 11 (2.67 eV). This indicates that at a higher PSS content, a larger number of SO₃⁻ groups from PSS is available to interact with PEDOT.¹³ However, at the EDOT : PSS weight ratio of 1 : 13, the band gap energy is higher at 2.72 eV due to the over-doping.⁵¹

For the effect of EDOT : Na₂S₂O₈ mole ratio, at the EDOT : PSS weight ratio of 1 : 11, the band gap energy of the EDOT : Na₂S₂O₈ mole ratio of 1 : 2 possessed the lowest value of 1.90 eV. This is due to the SO₄²⁻ ions from the oxidant interacting with the PEDOT chains as a dopant. This result is consistent with the increments in % PSS⁻ and % SO₄²⁻ determined by XPS. The doping process generally reduces the band gap energy between the HOMO and the LUMO to a level between 1–4 eV, as reported by Kar *et al.*, 2013.² However, the band gap energy for the EDOT : Na₂S₂O₈ mole ratio of 1 : 4 is larger because a large number of Na⁺ ions from the oxidant can interact with the PSS⁻ chains to form PSSNa,⁴⁴ which reduces the amount of doping sites on PSS. This result is consistent with the XPS result, indicating an increase in PSSNa, and the XRD result showing the highly crystalline peaks of PSSNa.

For the effect of surfactant type on the band gap energy of PEDOT:PSS, at the EDOT : PSS weight ratio of 1 : 11 and EDOT : Na₂S₂O₈ mole ratio of 1 : 2 utilizing Triton X-100 at 2.5CMC, this condition provided a band gap energy of 1.80 eV, which is lower than that of 3.00 eV for 2.5CMC SDS and 3.5 eV for 2.5CMC CTAB. Triton X-100 at 2.5CMC increases the HOMO level, allowing the polarons and bipolarons to delocalize.² CTAB and SDS provide higher band gap energies since they can

Table 2 Band gap and UV adsorption information

Sample code	E_g (eV)
Effect of PSS (no surfactant)	
EDOT : PSS weight ratio of 1 : 5 and EDOT : Na ₂ S ₂ O ₈ mole ratio of 1 : 1	2.92
EDOT : PSS weight ratio of 1 : 11 and EDOT : Na ₂ S ₂ O ₈ mole ratio of 1 : 1	2.67
EDOT : PSS weight ratio of 1 : 13 and EDOT : Na ₂ S ₂ O ₈ mole ratio of 1 : 1	2.72
Effect of oxidant (no surfactant)	
EDOT : PSS weight ratio of 1 : 11 and EDOT : Na ₂ S ₂ O ₈ mole ratio of 1 : 1	2.67
EDOT : PSS weight ratio of 1 : 11 and EDOT : Na ₂ S ₂ O ₈ mole ratio of 1 : 2	1.90
EDOT : PSS weight ratio of 1 : 11 and EDOT : Na ₂ S ₂ O ₈ mole ratio of 1 : 4	2.95
Effect of surfactant	
EDOT : PSS weight ratio of 1 : 11 and EDOT : Na ₂ S ₂ O ₈ mole ratio of 1 : 2 with Triton X-100 (at CMC)	2.39
EDOT : PSS weight ratio of 1 : 11 and EDOT : Na ₂ S ₂ O ₈ mole ratio of 1 : 2 with Triton X-100 (at 2.5CMC)	1.80
EDOT : PSS weight ratio of 1 : 11 and EDOT : Na ₂ S ₂ O ₈ mole ratio of 1 : 2 with Triton X-100 (at 3.5CMC)	2.83
EDOT : PSS weight ratio of 1 : 11 and EDOT : Na ₂ S ₂ O ₈ mole ratio of 1 : 2 with CTAB (at 2.5CMC)	3.50
EDOT : PSS weight ratio of 1 : 11 and EDOT : Na ₂ S ₂ O ₈ mole ratio of 1 : 2 with SDS (at 2.5CMC)	3.00



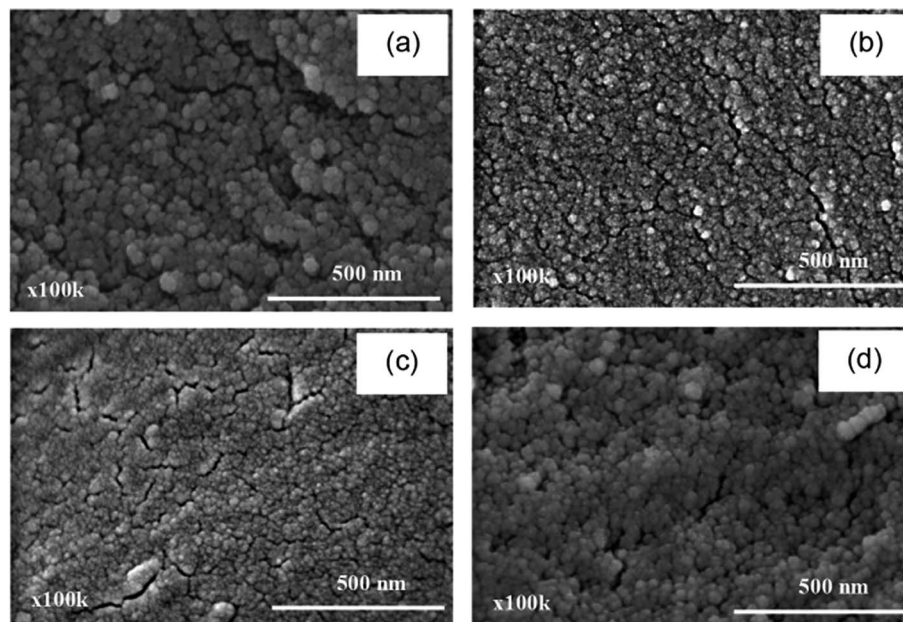


Fig. 5 PEDOT:PSS surface morphology at the EDOT : $\text{Na}_2\text{S}_2\text{O}_8$ mole ratio of 1 : 1 and at various EDOT : PSS weight ratios: EDOT : PSS weight ratio of (a) 1 : 1, (b) 1 : 5, (c) 1 : 11 and (d) 1 : 13.

obstruct the interaction of PSS with PEDOT, resulting in higher energy barriers between the HOMO and LUMO levels.

For the effect of Triton X-100 concentrations, a higher concentration provides a higher band gap energy above 2.5 eV, as shown in Table 2, where too many Triton X-100 molecules can obstruct the PEDOT and PSS interaction and form the TX-PSS complex, but can be removed by methanol washing.⁵⁴ The optimum Triton-X 100 concentration is 2.5CMC due to its lowest band gap energy (1.80 eV).

3.5 Morphology of PEDOT:PSS

The PEDOT:PSS morphology was investigated *via* FE-SEM. The effect of EDOT : PSS weight ratios at the EDOT : $\text{Na}_2\text{S}_2\text{O}_8$ mole ratio of 1 : 1 on the PEDOT:PSS morphology is shown in Fig. 5. The particle shapes are all spherical, as tabulated in Table 3. The PEDOT:PSS particle shapes were all spherical because PSS forms spherical micelles.⁵⁶ It can be noted that the packing parameter, $V_H/l_c a_0$, is less than 1/3 (where, V_H is the volume occupied by the hydrophobic groups in the micelle core, l_c is the length of the hydrophobic group in the core, and a_0 is the cross-sectional area occupied by the hydrophilic groups), indicating a spherical micelle.⁵⁷ The particle sizes of PEDOT:PSS at the EDOT : PSS weight ratios of 1 : 1, 1 : 5, 1 : 11, and 1 : 13 are 33.20 ± 4.29 , 16.57 ± 1.99 , 16.26 ± 1.40 , and 17.19 ± 2.05 nm, respectively, as tabulated in Table 3. The particle size of PEDOT:PSS decreased with an increase in PSS because PSS is an anionic surfactant,⁵⁸ which forms PSS micelles at the CMC of 7×10^{-5} mol L^{-1} . The EDOT : PSS weight ratio of 1 : 5 is the condition of 4.75CMC PSS, and thus the average particle size of PEDOT:PSS became smaller. Above the EDOT : PSS weight ratio of 1 : 5, the particle size of PEDOT:PSS is not significantly different.

For the effect of EDOT : $\text{Na}_2\text{S}_2\text{O}_8$ mole ratio at the EDOT : PSS weight ratio of 1 : 11, the particle shapes and sizes are tabulated in Table 3. The particle sizes of PEDOT:PSS at the weight ratio of 1 : 11 and EDOT : $\text{Na}_2\text{S}_2\text{O}_8$ mole ratios of 1 : 1, 1 : 1.5, 1 : 2, 1 : 2.5, 1 : 3, and 1 : 4 are 16.26 ± 1.40 , 17.28 ± 2.07 , 19.84 ± 2.36 , 21.82 ± 2.36 , 22.95 ± 2.20 , and 23.97 ± 3.48 nm, respectively. The particle size of PEDOT:PSS increased monotonically with an increase in EDOT : $\text{Na}_2\text{S}_2\text{O}_8$ mole ratio. This result is possibly derived from many successive steps: a larger oxidant amount yields a faster nucleation rate for EDOT radical ions; PEDOT chains are polymerized with a lower molecular weight; easier access into PSS micelles leads to a larger EDOT content in a given PSS micelle volume; and PEDOT chains aggregate to form a larger particle size. Additionally, the oxidant ions (Na^+ and SO_4^{2-}) can reduce the electro-repulsion among the SO_3^- groups of the PSS micelle, leading to an increase in the PSS micelle size, consistent with the effect of salt ions on SDS micelles, as reported by Kim *et al.*, 2001.⁵⁹ The result can be clearly observed in the FE-SEM images of PEDOT:PSS at the EDOT : $\text{Na}_2\text{S}_2\text{O}_8$ mole ratios of 1 : 1 and 1 : 2, as shown in Fig. 5(c) and 6(a), respectively.

The effect of surfactant type on the PEDOT:PSS morphology at the EDOT : PSS weight ratio of 1 : 11 and the EDOT : $\text{Na}_2\text{S}_2\text{O}_8$ mole ratio of 1 : 2 using CTAB (cationic surfactant), SDS (anionic surfactant), and Triton X-100 (non-ionic surfactant) at 2.5CMC is shown in Fig. 6(b)–(d), respectively. The particle shapes and sizes of the synthesized PEDOT:PSS are tabulated in Table 3. The shapes of PEDOT:PSS in the three surfactant systems are spherical. The particle size of PEDOT:PSS without surfactant is smaller than that with the surfactants since the PSS micelles are likely disturbed by the surfactant molecules. Among the surfactants, PEDOT:PSS synthesized with CTAB at

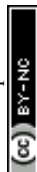


Table 3 The electrical conductivity, shape, and size of PEDOT:PSS synthesized under various conditions

Sample code EDOT : PSS and EDOT : Na ₂ S ₂ O ₈	Electrical conductivity (S cm ⁻¹)	Particle shape	Particle size
Effect of PSS (no surfactant)			
wt ratio 1 : 1 and mole ratio 1 : 1	452.81 ± 31.59	Spherical	33.20 ± 4.29
wt ratio 1 : 3 and mole ratio 1 : 1	366.55 ± 28.82	Spherical	32.88 ± 2.88
wt ratio 1 : 5 and mole ratio 1 : 1	250.23 ± 85.13	Spherical	16.57 ± 1.99
wt ratio 1 : 7 and mole ratio 1 : 1	477.17 ± 36.97	Spherical	16.60 ± 1.77
wt ratio 1 : 9 and mole ratio 1 : 1	828.01 ± 81.77	Spherical	16.75 ± 2.81
wt ratio 1 : 11 and mole ratio 1 : 1	999.74 ± 10.86	Spherical	16.26 ± 1.40
wt ratio 1 : 13 and mole ratio 1 : 1	524.23 ± 42.29	Spherical	17.19 ± 2.05
Effect of oxidant (no surfactant)			
wt ratio 1 : 11 and mole ratio 1 : 1	999.74 ± 10.86	Spherical	16.26 ± 1.40
wt ratio 1 : 11 and mole ratio 1 : 1.5	1048.78 ± 35.10	Spherical	17.28 ± 2.07
wt ratio 1 : 11 and mole ratio 1 : 2	1556.85 ± 46.84	Spherical	19.84 ± 2.36
wt ratio 1 : 11 and mole ratio 1 : 2.5	564.71 ± 53.44	Spherical	21.82 ± 2.36
wt ratio 1 : 11 and mole ratio 1 : 3	199.46 ± 37.51	Spherical	22.95 ± 2.20
wt ratio 1 : 11 and mole ratio 1 : 4	55.61 ± 0.10	Spherical	23.97 ± 3.48
Effect of surfactant			
wt ratio 1 : 11 and mole ratio 1 : 2 with CTAB (at CMC)	12.43 ± 1.33	Spherical	24.98 ± 2.54
wt ratio 1 : 11 and mole ratio 1 : 2 with CTAB (at 2.5CMC)	0.41 ± 0.06	Spherical	24.46 ± 2.35
wt ratio 1 : 11 and mole ratio 1 : 2 with CTAB (at 10CMC)	29.82 ± 13.02	Spherical	20.91 ± 2.91
wt ratio 1 : 11 and mole ratio 1 : 2 with SDS (at CMC)	13.23 ± 4.45	Spherical	23.73 ± 3.49
wt ratio 1 : 11 and mole ratio 1 : 2 with SDS (at 2.5CMC)	25.04 ± 5.48	Spherical	44.01 ± 9.14
wt ratio 1 : 11 and mole ratio 1 : 2 with SDS (at 10CMC)	45.12 ± 6.02	Spherical	26.44 ± 7.16
wt ratio 1 : 11 and mole ratio 1 : 2 with Triton X-100 (at CMC)	1289.43 ± 81.14	Spherical	21.37 ± 3.05
wt ratio 1 : 11 and mole ratio 1 : 2 with Triton X-100 (at 2.5CMC)	1879.49 ± 13.87	Spherical	56.77 ± 5.54
wt ratio 1 : 11 and mole ratio 1 : 2 with Triton X-100 (at 3.5CMC)	328.69 ± 35.90	Spherical	36.48 ± 4.30
wt ratio 1 : 11 and mole ratio 1 : 2 with Triton X-100 (at 5CMC)	298.92 ± 1.49	Spherical	33.95 ± 4.07
wt ratio 1 : 11 and mole ratio 1 : 2 with Triton X-100 (at 10CMC)	238.87 ± 4.04	Spherical	30.28 ± 3.62

2.5CMC showed the smallest particle size of 24.46 ± 2.35 nm since the electro-attractive force between the cationic CTAB surfactant and PSS⁻ disturbs the formation of PSS micelles.⁵³

For the anionic surfactant SDS at 2.5CMC, the particle size of PEDOT:PSS is 44.01 ± 9.14 nm, and SDS can repel and replace PSS⁻; thus, disturbing the formation of PSS micelles.³⁷ For the



Fig. 6 PEDOT:PSS surface morphology at the EDOT : PSS weight ratio of 1 : 11 and EDOT : Na₂S₂O₈ mole ratio of 1 : 2 using various surfactant types: (a) no surfactant, (b) CTAB (2.5CMC), (c) SDS (2.5CMC), and (d) Triton X-100 (2.5CMC).



non-ionic surfactant Triton X-100 at 2.5CMC, the particle size of PEDOT:PSS was the largest at 56.77 ± 5.54 nm since Triton X-100 interferes with the PSS micelle formation. Triton X-100 consists of a large ethoxy chain acting as a bulky polar head group, which can separate the SO_3^- groups of the PSS micelle; thus, reducing the electrostatic repulsive interaction, leading to an increase in the PSS micelle size.⁶⁰

The effect of surfactant concentration at the EDOT : PSS weight ratio of 1 : 11 and EDOT : $\text{Na}_2\text{S}_2\text{O}_8$ mole ratio of 1 : 2 on the PEDOT:PSS morphology is shown in Table 3. The shapes of PEDOT:PSS are still spherical. At the CMC, the surfactants form micelles, which are unstable and can disturb the interaction between PEDOT and PSS; thus, the particle sizes are larger than PEDOT:PSS without a surfactant.³⁰ Above the CMC, surfactants are prone to interact with the PSS molecules, and thus the formation of PSS micelles is interrupted, leading to larger particle sizes.

3.6 Thermal stability

The thermal stability of PEDOT:PSS was investigated by TG-DTA under an N_2 flow, as shown in Fig. 7, and the onset decomposition temperatures ($T_{d,\text{onset}}$) of PEDOT:PSS with different surfactant systems were measured. The $T_{d,\text{onset}}$ of PEDOT:PSS at the EDOT : PSS weight ratio of 1 : 11 and EDOT : $\text{Na}_2\text{S}_2\text{O}_8$ mole ratio of 1 : 2 without surfactant was 499 °C and the char yield at 790 °C was 53.43%. The $T_{d,\text{onset}}$ of PEDOT:PSS synthesized under the same conditions using Triton X-100 at 2.5CMC was 492.97 °C and the char yield at 790 °C was 44.05%. For the CTAB system (2.5CMC), the $T_{d,\text{onset}}$ of PEDOT:PSS was 407.98 °C and the char yield at 790 °C was 51.62%. For the SDS system (2.5CMC), the $T_{d,\text{onset}}$ of PEDOT:PSS was 413.52 °C and the char yield at 790 °C was 50.52%. The PEDOT:PSS with the surfactants possessed lower $T_{d,\text{onset}}$ and % char yield values than that without surfactant. Thus, PEDOT:PSS with the surfactants possessed higher thermal degradation values because the surfactants disturbed the polymerization of PEDOT:PSS, resulting in a shorter conjugated polymer.⁶¹ For the PEDOT:PSS

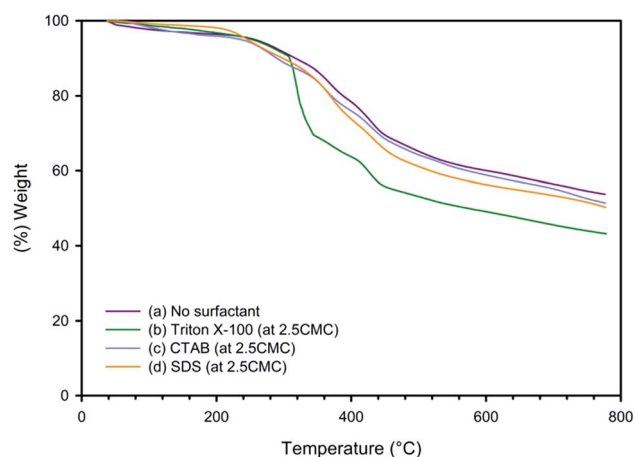


Fig. 7 TGA spectra of PEDOT:PSS at the EDOT : PSS weight ratio of 1 : 11 and EDOT : $\text{Na}_2\text{S}_2\text{O}_8$ mole ratio of 1 : 2: (a) no surfactant, (b) Triton X-100 (2.5CMC), (c) CTAB (2.5CMC) and (d) SDS (2.5CMC).

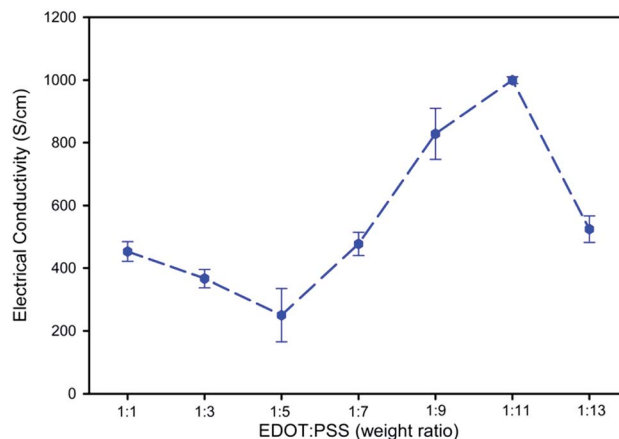


Fig. 8 Electrical conductivity of PEDOT:PSS at the EDOT : $\text{Na}_2\text{S}_2\text{O}_8$ mole ratio of 1 : 1 and at various EDOT : PSS weight ratios.

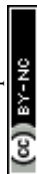
without surfactant and with Triton X-100, CTAB, and SDS, the thermograms show four decomposition stages: the first stage is the decomposition of water and moisture in the temperature range of 100–180 °C; the second stage is the decomposition of the side chains in the temperature range of 180–320 °C; the third stage exhibits the decomposition of PSS in the temperature range of 320–400 °C; and the last stage illustrates the decomposition of PEDOT (main chain) in the temperature range of 400–790 °C.²³ For the effect of EDOT : $\text{Na}_2\text{S}_2\text{O}_8$ mole ratio at the EDOT : PSS weight ratio of 1 : 11, the TGA thermograms were nearly the same as the above results.

3.7 Electrical conductivity

The electrical conductivity of the PEDOT:PSS synthesized at the EDOT : $\text{Na}_2\text{S}_2\text{O}_8$ mole ratio of 1 : 1 and at various EDOT : PSS weight ratios is shown in Fig. 8. For EDOT : PSS weight ratios between 1 : 1 and 1 : 5, the electrical conductivity of PEDOT:PSS decreased from 452.81 ± 31.59 to 250.23 ± 85.13 S cm^{-1} since the PSS amount is low and it may act as an insulator.²⁰ At EDOT : PSS weight ratios between 1 : 5 and 1 : 11, the electrical



Fig. 9 Electrical conductivity of PEDOT:PSS at the EDOT : PSS weight ratio of 1 : 11 and at various EDOT : $\text{Na}_2\text{S}_2\text{O}_8$ mole ratios.



conductivity of PEDOT:PSS increased from 250.23 ± 85.13 to 999.74 ± 10.86 S cm⁻¹ since PSS acts effectively as a dopant.¹³ The electrical conductivity increases due to an increase in the number of charge carriers.⁵² This finding is consistent with the increase in % PSS⁻ and % SO₄²⁻ from XPS and the decrease in the band gap energy from UV-Vis. However, at the EDOT : PSS weight ratio of 1 : 13, the electrical conductivity of PEDOT:PSS decreased to 524.23 ± 42.29 S cm⁻¹ due to over-doping.⁵¹ Hence, the EDOT : PSS weight ratio of 1 : 11 is optimal owing to the highest electrical conductivity obtained (999.74 ± 10.86 S cm⁻¹).

The electrical conductivity of PEDOT:PSS using the EDOT : PSS weight ratio of 1 : 11 at various EDOT : Na₂S₂O₈ mole ratios is shown in Fig. 9. As the EDOT : Na₂S₂O₈ mole ratio increased from 1 : 1 to 1 : 2, the electrical conductivity of PEDOT:PSS increased from 999.74 ± 10.86 to 1556.85 ± 46.84 S cm⁻¹ since SO₄²⁻ from the oxidant may also act as a dopant¹² by interacting with the oxidized PEDOT chain. This finding is consistent with the % SO₄²⁻ increase from XPS, the decrease in band gap energy, and the low PSSNa amount. At EDOT : Na₂S₂O₈ mole ratios above 1 : 2, the electrical conductivity of PEDOT:PSS decreased from 1556.85 ± 46.84 S cm⁻¹ to 55.61 ± 0.10 S cm⁻¹ because Na⁺ ions from the oxidant can react with PSS⁻ to form PSSNa, which reduces the amount of PSS

available to dope PEDOT, leading to a decrease in electrical conductivity.⁴² The increase in PSSNa was identified at the EDOT : Na₂S₂O₈ mole ratios of 1 : 3 and 1 : 4 by XPS and XRD. Moreover, the decrease in electrical conductivity is related to the increase in the band gap energy. Thus, the EDOT : Na₂S₂O₈ mole ratio of 1 : 2 is optimal to acquire the high PEDOT:PSS electrical conductivity of 1556.85 ± 46.84 S cm⁻¹, as confirmed by the low band gap energy of 1.90 eV compared to other EDOT : Na₂S₂O₈ mole ratios.

The electrical conductivity of PEDOT:PSS synthesized using the EDOT : PSS weight ratio of 1 : 11 and EDOT : Na₂S₂O₈ mole ratio of 1 : 2 with various surfactant types and concentrations is shown in Fig. 10. The CTAB and SDS systems are not suitable to synthesize PEDOT:PSS since the electrical conductivity is 100 times lower than that of PEDOT:PSS without these two surfactants. CTAB can react with the PSS chain,⁵³ whereas, SDS can replace PSS.³⁷ Moreover, these two systems induce a decrease in the amount of dopant (% SO₃⁻ of PSS and % SO₄²⁻ of Na₂S₂O₈), as confirmed by XPS and the increase in band gap energy from 1.90 eV to 3.50 eV for CTAB and 1.90 eV to 3.00 eV for SDS. For Triton X-100, it can react with both PEDOT and the PSS chains, and can form a TX-PSS complex, which can be easily removed by methanol washing,⁵⁴ resulting in the removal of PSS⁻ acting as a dopant and PSSNa as a salt. This suggests that Triton X-100 reduces the PEDOT and PSS interaction as well as the PSSNa amount. From the XPS result, the decrease in the amount of PSSNa amount was clearly observed with an increase Triton X-100 concentration together with a decrease in the amount of dopant (% SO₃⁻ of PSS and % SO₄²⁻ of Na₂S₂O₈). However, using Triton X-100 at 2.5CMC provides a suitable condition for the removal of PSSNa since the highest electrical conductivity of 1879.49 ± 13.87 S cm⁻¹ with the lowest band gap energy of 1.80 eV were obtained, while the dopant amount remained high. A higher Triton X-100 concentration tended to remove the dopants, although PSSNa was preferentially eliminated.

To confirm the electrical conductivity of the synthesized PEDOT:PSS as measured by a custom-built 2-point probe, the electrical conductivity of graphite (particle size < 20 μm, Sigma Aldrich) and multi-walled carbon nanotubes (specific of diameter of 30–50 nm, >95 wt% purity, Alphanano Technology Co., Ltd.) was also measured by using the same equipment and the same sample thickness. The obtained electrical conductivity of

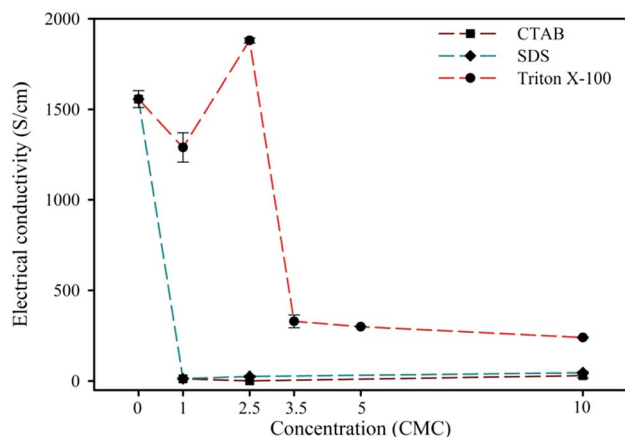


Fig. 10 Electrical conductivity of PEDOT:PSS at the EDOT : PSS weight ratio of 1 : 11 and EDOT : Na₂S₂O₈ mole ratio of 1 : 2 with various surfactant types and concentrations.

Table 4 Comparison of the electrical conductivity, particle shape, and size of various PEDOT:PSS particles

Sample	Oxidant	Electrical conductivity (S cm ⁻¹)	Particle shape	Particle size (nm)	Reference
PEDOT:PSS	Fe(NO ₃) ₃ · 9H ₂ O	9.90	—	—	Qi <i>et al.</i> , 1998
PEDOT:PSS	Fe(NO ₃) ₃ · 9H ₂ O	2.50	—	—	Lefebvre <i>et al.</i> , 1998
	FeCl ₃	0.006	—	—	
PEDOT:PSS	Fe(NO ₃) ₃ · 9H ₂ O	1.50	—	—	Lefebvre <i>et al.</i> , 1999
PEDOT:PSS	Fe(NO ₃) ₃ · 9H ₂ O	4.30	—	—	Dai <i>et al.</i> , 2008
PEDOT:PSS	Na ₂ S ₂ O ₈	27.50	Irregular	3000	Wichiansee <i>et al.</i> , 2008
PEDOT:PSS	Na ₂ S ₂ O ₈	11.69	Irregular	3400	Chanthanont <i>et al.</i> , 2013
PEDOT:PSS	Na ₂ S ₂ O ₈	1556.85	Spherical	19.84	Present work
PEDOT:PSS with Triton X-100 at 2.5CMC	Na ₂ S ₂ O ₈	1879.49	Spherical	56.77	



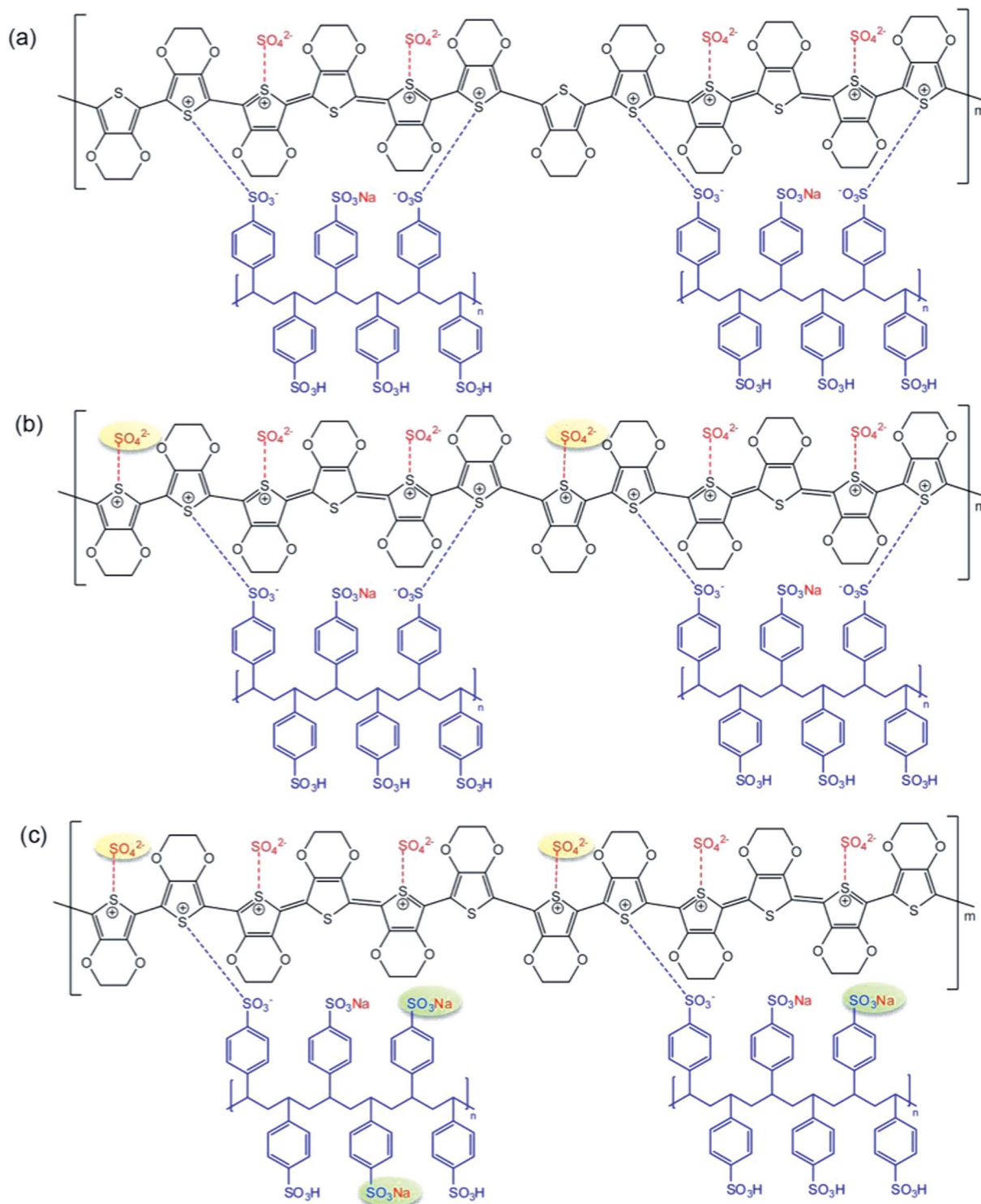


Scheme 2 Proposed interaction of PEDOT:PSS at the EDOT : Na₂S₂O₈ mole ratio of 1 : 1 and various EDOT : PSS weight ratios: at an EDOT : PSS weight ratio (a) lower than 1 : 11, (b) 1 : 11, where more PSS interact, and (c) higher than 1 : 11 with a higher PSSNa amount to reduce the doping sites on PSS.

graphite was 14 282.18 S cm⁻¹ (ref. 62) and MWCNT was 1589.17 S cm⁻¹,⁶³ consistent with the data from previous work. It should be noted that the electrical conductivity of the synthesized PEDOT:PSS powder was in the same range as that of MWCNT.

The related works of the synthesized PEDOT:PSS powder are tabulated in Table 4, where Qi and co-workers (1998) prepared PEDOT:PSS *via* chemical oxidative polymerization. They used EDOT and PSSNa as the reactants and Fe(NO₃)₃·9H₂O as the oxidant. The reaction time was 2 h to obtain a dark blue



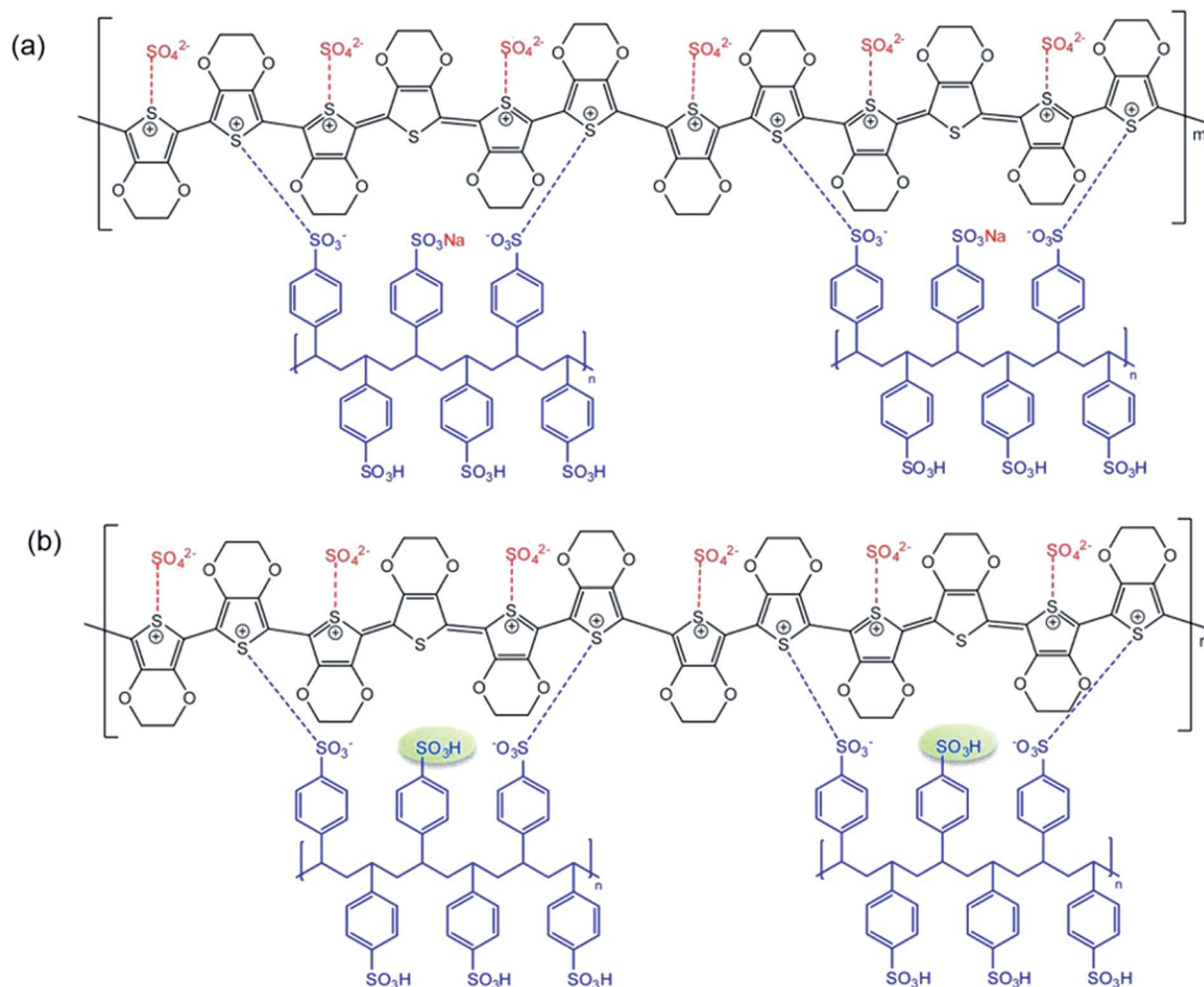


Scheme 3 Proposed structure of PEDOT:PSS at the EDOT : PSS weight ratio of 1 : 11 and at various EDOT : Na₂S₂O₈ mole ratios: at an EDOT : Na₂S₂O₈ mole ratio (a) lower than 1 : 2, (b) 1 : 2, where SO₄²⁻ acts as a secondary dopant and (c) higher than 1 : 2, where a higher PSSNa amount is generated.

solution. The electrical conductivity of PEDOT:PSS was 9.9 S cm⁻¹.⁶⁴ Lefebvre *et al.* synthesized PEDOT:PSS using a mixed solvent of acetonitrile : water at a ratio of 1 : 1. EDOT and NaPSS were used as the reactants and Fe(NO₃)₃·9H₂O and FeCl₃ were used the oxidants. The electrical conductivity value

at the EDOT : Fe(NO₃)₃·9H₂O mole ratio of 1 : 5 was 2.50 S cm⁻¹, while at the EDOT : FeCl₃ mole ratio of 1 : 10 it was 0.006 S cm⁻¹.²⁴ Lefebvre *et al.* prepared PEDOT:PSS using Fe(NO₃)₃·9H₂O as the oxidant and a mixture of acetonitrile : water at a ratio of 1 : 1 as the solvent. Using the





Scheme 4 Proposed structure of PEDOT:PSS at the EDOT : PSS weight ratio of 1 : 11 and EDOT : $\text{Na}_2\text{S}_2\text{O}_8$ mole ratio of 1 : 2: (a) no surfactant; and (b) Triton X-100, where PSSNa amount is reduced through methanol washing.

EDOT : $\text{Fe}(\text{NO}_3)_3 \cdot 9\text{H}_2\text{O}$ mole ratio of 1 : 10, the electrical conductivity was 1.50 S cm^{-1} .²¹ Dai *et al.*, 2008, synthesized PEDOT:PSS using $\text{Fe}(\text{NO}_3)_3 \cdot 9\text{H}_2\text{O}$ as the oxidant and water as the solvent and the reaction time was 24 h at room temperature, giving an electrical conductivity value of 4.3 S cm^{-1} .⁶⁵ Wichiansee and co-worker prepared PEDOT:PSS by mixing EDOT, PSS, and $\text{Na}_2\text{S}_2\text{O}_8$ in distilled water. Subsequently, $\text{Fe}_2(\text{SO}_4)_3$ was added to the solution and it was stirred continuously for 24 h. The electrical conductivity was 27.50 S cm^{-1} .²² Chanthanont and co-workers, 2013, synthesized PEDOT:PSS using an EDOT : PSS mole ratio of 1 : 1 in distilled water. $\text{Na}_2\text{S}_2\text{O}_8$ was used as the oxidant and $\text{Fe}_2(\text{SO}_4)_3$ was added to the solution and stirred vigorously for 24 h. The electrical conductivity was 11.69 S cm^{-1} .²³

3.8 Interaction of PEDOT:PSS and dopants including PSSNa

For the effect of EDOT : PSS weight ratio, at the EDOT : $\text{Na}_2\text{S}_2\text{O}_8$ mole ratio of 1 : 1, PSS as the dopant reacts with PEDOT, as shown in Scheme 2.¹³ At an EDOT : PSS weight ratio lower than 1 : 11, as shown in Scheme 2(a), a small amount of PSS interacts

with PEDOT, as confirmed by XPS. At the EDOT : PSS weight ratio of 1 : 11, as shown in Scheme 2(b), more PSS chains are available to dope the PEDOT chains. However, at a EDOT : PSS weight ratio above 1 : 11, as shown in Scheme 2(c), PSS also reacts with Na^+ from $\text{Na}_2\text{S}_2\text{O}_8$ to form PSSNa on PSS, as confirmed by XPS and XRD. The presence of PSSNa reduces the number of doping sites on PSS. Hence, the EDOT : PSS weight ratio of 1 : 11 is the optimal condition because of the highest electrical conductivity ($999.74 \pm 10.86 \text{ S cm}^{-1}$) and lowest UV-Vis energy gap (2.67 eV). This shows that only a proper amount of PSS increases the number of charge carriers, resulting in an increase in the electrical conductivity.⁵²

The PEDOT:PSS synthesized at the EDOT : PSS weight ratio of 1 : 11 and various EDOT : $\text{Na}_2\text{S}_2\text{O}_8$ mole ratios is demonstrated in Scheme 3. At an EDOT : $\text{Na}_2\text{S}_2\text{O}_8$ mole ratio lower than 1 : 2, as shown in Scheme 3(a), SO_4^{2-} acts as an oxidant and dopant¹² and it interacts with the PEDOT chains, but a small number of SO_4^{2-} ions are available to interact with PEDOT to generate a small number of charge carriers, resulting in low electrical conductivity.⁵² In addition, Na^+ from $\text{Na}_2\text{S}_2\text{O}_8$ also reacts with PSS to form PSSNa, as verified by XPS and XRD.



At the EDOT : Na₂S₂O₈ mole ratio of 1 : 2, as shown in Scheme 3(b), more SO₄²⁻ ions are available to interact with PEDOT, as confirmed by XPS, while the PSSNa amount does not significantly increase. At an EDOT : Na₂S₂O₈ mole ratio above 1 : 2, as shown in Scheme 3(c), more SO₄²⁻ ions interact with PEDOT, but at the expense of more Na⁺ ions from Na₂S₂O₈ reacting with PSS to form PSSNa, as confirmed by XPS and XRD. Therefore, the EDOT : Na₂S₂O₈ mole ratio of 1 : 2 is the optimal condition since it provides the highest electrical conductivity (1556.85 ± 46.84 S cm⁻¹) and lowest energy gap of 1.90 eV.

At the EDOT : PSS weight ratio of 1 : 11 and EDOT : Na₂S₂O₈ mole ratio of 1 : 2, the interactions are shown in Scheme 4(a) without a surfactant and in Scheme 4(b) with Triton X-100. As shown in Scheme 4(b), Triton X-100 reacts with PSS and it reduces the PEDOT and PSS interaction and the PSSNa amount, which can be easily removed by methanol washing,⁵⁴ as verified by XPS. Hence, using Triton X-100 at 2.5CMC yielded the highest electrical conductivity of 1879.49 ± 13.87 S cm⁻¹ with the lowest energy gap of 1.80 eV.

4. Conclusion

PEDOT:PSS was successfully synthesized *via* chemical oxidative polymerization with high electrical conductivity and a systematic route was used to investigate the effects of EDOT : PSS weight ratio, EDOT : Na₂S₂O₈ mole ratio, and surfactant type and concentration on its properties. The EDOT : PSS weight ratio of 1 : 11 provided the highest PSS⁻ dopant amount to interact with PEDOT. For the effect of EDOT : Na₂S₂O₈ mole ratio, the EDOT : Na₂S₂O₈ mole ratio of 1 : 2 was the optimal condition since SO₄²⁻ from the oxidant acting as a secondary dopant increased the number of charge carriers, resulting in the high electrical conductivity of 1556.85 ± 46.84 S cm⁻¹ and low energy gap of 1.90 eV. In the case of the three surfactant systems, Triton X-100 (2.5CMC) was the suitable surfactant to synthesize PEDOT:PSS, at the EDOT : PSS weight ratio of 1 : 11 and EDOT : Na₂S₂O₈ mole ratio of 1 : 2 because of the highest electrical conductivity of 1879.49 ± 13.87 S cm⁻¹ and the lowest energy gap of 1.80 eV. Triton X-100 molecules reduced the PEDOT and PSS interactions and the amount of PSSNa, which could be easily removed by methanol washing. The washing reduced the PSSNa amount on PSS, which then provided a higher number of doping sites on PSS. The particle shape of the PEDOT:PSS synthesized in all conditions were spherical. The particle size of PEDOT:PSS varied from 16.57 ± 1.99 to 56.77 ± 5.54 nm. The thermogravimetric analysis revealed that PEDOT:PSS with surfactants exhibited lower thermal stability than PEDOT:PSS without surfactant. The synthesis of PEDOT:PSS in this work provides guidance for the production and use of PEDOT:PSS particles in powder form with very high electrical conductivity, potentially suitable for many electronic applications such as drug delivery, thin film transistors, light emitting diodes, sensors, photovoltaics, and actuators.

Conflicts of interest

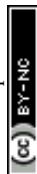
There are no conflicts to declare.

Acknowledgements

The authors are grateful for the scholarship from the Thailand Research Fund through the Royal Golden Jubilee PhD Program (RGJ PHD/0108/2559), the funding from the Conductive and Electroactive Polymer Research Unit, the Thailand Research Fund (TRF), and the Royal Thai Government.

References

- 1 T. H. Le, Y. Kim and H. Yoon, *Polymers*, 2017, **9**, 150.
- 2 P. Kar, *Doping in conjugated polymers*, Scrivener Publishing LLC, Canada, 1st edn, 2013.
- 3 H. Shirakawa, E. J. Louis, A. G. MacDiarmid, C. K. Chiang and A. J. Heeger, *J. Chem. Soc., Chem. Commun.*, 1997, 578–580.
- 4 N. Hall, *Chem. Commun.*, 2003, 1–4.
- 5 W. S. Huang, B. D. Humphrey and A. G. MacDiarmid, *J. Chem. Soc., Faraday Trans. 1*, 1986, **82**, 2385–2400.
- 6 R. D. McCullough, R. D. Lowe, M. Jayaraman and D. L. Anderson, *J. Org. Chem.*, 1993, **58**, 904–912.
- 7 L. Dai, B. Winkler, L. Dong, L. Tong and W. H. A. Mau, *Adv. Mater.*, 2001, **13**, 915–925.
- 8 H. E. Katz, *J. Mater. Chem.*, 1997, **7**, 369–376.
- 9 M. Hiraoka, P. Fiorini, J. O'Callaghan, I. Yamashita, C. V. Hoof and M. Op de Beeck, *Sens. Actuators, A*, 2012, **177**, 23–29.
- 10 K. Yan, Z.-X. Liu, X. Li, J. Chen, H. Chen and C.-Z. Li, *Org. Chem. Front.*, 2018, **5**, 2845.
- 11 D. Svirskis, J. Travas-Sejdic, A. Rodgers and S. Garg, *J. Controlled Release*, 2010, **146**, 6–15.
- 12 N. Paradee and A. Sirivat, *Polym. Int.*, 2013, **63**, 106–113.
- 13 L. Ouyang, C. Musumeci, M. J. Jafari, T. Ederth and O. Inganäs, *ACS Appl. Mater. Interfaces*, 2015, **7**, 19764–19773.
- 14 A. Cho, S. Kim, S. Kim, W. Cho, C. Park, F. S. Kim and J. H. Kim, *J. Polym. Sci., Part B: Polym. Phys.*, 2016, **54**, 1530–1536.
- 15 K. Muro, M. Watanabe, T. Tamai, K. Yazawa and K. Matsukawa, *RSC Adv.*, 2016, **6**, 87147–87152.
- 16 C. Liu, F. Jiang, M. Huang, R. Yue, B. Lu, J. Xu and G. Liu, *J. Electron. Mater.*, 2011, **40**, 648–651.
- 17 S. Lim, S. H. Park, T. K. An, H. S. Lee and S. H. Kim, *RSC Adv.*, 2015, **6**, 2004–2010.
- 18 J. Ouyang, Q. Xu, C.-W. Chu, Y. Yang, G. Li and J. Shinar, *Polymer*, 2004, **45**, 8443–8450.
- 19 J. Y. Oh, M. Shin, J. B. Lee, J. H. Ahn, H. K. Baik and U. Jeong, *ACS Appl. Mater. Interfaces*, 2014, **6**, 6954–6961.
- 20 T. Horii, H. Hikawa, Y. Mochizuki and H. Okuzaki, *Trans. Mater. Res. Soc. Jpn.*, 2012, **37**, 515–518.
- 21 M. C. Lefebvre, Z. Qi and P. G. Pickup, *J. Electrochem. Soc.*, 1999, **146**, 2054–2058.
- 22 W. Wichiansee and A. Sirivat, *Materials Science and Engineering C.*, 2008, **29**, 78–84.
- 23 P. Chanthanont and A. Sirivat, *Polym. Adv. Technol.*, 2013, **32**, 21367.



- 24 M. Lefebvre, Z. Qi, D. Rana and P. G. Pickup, *J. Electrochem. Soc.*, 1999, **146**, 2054–2058.
- 25 S. Khan and A. K. Narula, *Eur. Polym. J.*, 2016, **81**, 161–172.
- 26 Polypyrrole Stability and Coatings for Radar Absorbing Materials, 2004, <http://www.dtic.mil/dtic/tr/fulltext/u2/a436251.pdf>.
- 27 Z. Fufang, Z. Baogai, S. Zhuoran, H. Yuanming and P. Chanxu, *Key Eng. Mater.*, 2009, **407–408**, 573–576.
- 28 N. Sangiorgi, L. Aversa, R. Tatti, R. Verucchi and A. Sanson, *Opt. Mater.*, 2016, **64**, 18–27.
- 29 T. Permpool, A. Sirivat and D. Aussawasathien, *Polym. Int.*, 2014, **63**, 2076–2083.
- 30 K. Phasuksom and A. Sirivat, *Synth. Met.*, 2016, **219**, 142–153.
- 31 C. Liang and H.-W. Su, *Ind. Eng. Chem. Res.*, 2009, **48**, 5558–5562.
- 32 C. Coletta, Z. Cui, A. Dazzi, J. M. Guigner, S. Neron, J.-L. Marignier and S. Remita, *Radiat. Phys. Chem.*, 2016, **126**, 21–31.
- 33 N. D. Koromilas, G. C. Lainioti, E. K. Oikonomou, G. Bokias and J. K. Kallitsis, *Eur. Polym. J.*, 2014, **54**, 39–51.
- 34 E. G. Langford, K. D. Shaughnessy, T. C. Devore, D. Lawrence and C. Constantin, *MRS Adv.*, 2016, **1**, 465–469.
- 35 C. Sriprachubwong, C. Karuwan, A. Wisitsoratt, D. Phokharatkul, T. Lomas, P. Sritongkham and A. Tuantranont, *J. Mater. Chem.*, 2012, **22**, 5478–5485.
- 36 C. Lin, B. Fan, J. X. Zhang, X. Yang and H. Zhang, *Desalin. Water Treat.*, 2015, **57**, 21627–21733.
- 37 C. Yeon, G. Kim, J. W. Lim and S. J. Yun, *RSC Adv.*, 2017, **7**, 5888–5897.
- 38 K. Sukchol, S. Thongyai, P. Praserttham and G. A. Sotzing, *Synth. Met.*, 2013, **179**, 10–17.
- 39 T.-R. Chou, S.-H. Chen, Y.-T. Chiang, T.-T. Chang, C.-W. Lin and C.-Y. Chao, *Org. Electron.*, 2017, **48**, 223–229.
- 40 T. G. Kim, S. R. Ha, H. Choi, K. Uh, U. Kundapur, S. Park, C. W. Lee, S. Lee, J. Kim and J.-M. Kim, *ACS Appl. Mater. Interfaces*, 2017, **9**, 19231–19237.
- 41 C. Yeon, S. J. Yun, J. Kim and J. W. Lim, *Adv. Electron. Mater.*, 2015, **1**, 1500121.
- 42 Y. Xia and J. Ouyang, *Macromolecules*, 2009, **42**, 4141–4147.
- 43 G. Zotti, S. Zecchin, G. Schiavon, F. Louwet, L. Groenendaal, X. Crispin, W. Osikowicz, W. Salaneck and M. Fahlman, *Macromolecules*, 2003, **36**, 3337–3344.
- 44 M. Chen, K. Shafer-Peltier, S. J. Randtke and E. Peltier, *Chem. Eng. J.*, 2018, **344**, 155–164.
- 45 H. Park, S. H. Lee, F. S. Kim, H. H. Choi, I. W. Cheong and J. H. Kim, *J. Mater. Chem. A*, 2014, **2**, 6532–6539.
- 46 L. Zhang, H. Deng, S. Liu, Q. Zhang, F. Chen and Q. Fu, *RSC Adv.*, 2015, **5**, 105592–105599.
- 47 A. B. Volynsky, A. Y. Stakheev, N. S. Telegina, V. G. Senin, L. M. Kustov and R. Wennirch, *Spectrochim. Acta, Part B*, 2001, **56**, 1387–1396.
- 48 J. Zhao, S. Xu, K. Tschulik, R. G. Compton, M. Wei, D. O'Hare, D. G. Evans and X. Duan, *Adv. Funct. Mater.*, 2015, **25**, 2745–2753.
- 49 S. Fabiano, S. Braun, X. Liu, E. Weverberghs, P. Gerbaux, M. Fahlman, M. Berggren and X. Crispin, *Adv. Mater.*, 2014, **26**, 6000–6006.
- 50 L. Qie, W. Chen, X. Xiong, C. Hu, F. Zou, P. Hu and Y. Huang, *Adv. Sci.*, 2015, **2**, 1500195.
- 51 P. Tehrani, A. Kanciurowska, X. Crispin, N. D. Robinson, M. Fahlman and M. Berggren, *Solid State Ionics*, 2007, **177**, 3521–3527.
- 52 T.-C. Tsai, H.-C. Chang, C.-H. Chen and W.-T. Whang, *Org. Electron.*, 2011, **12**, 2159–2164.
- 53 B. Fan, X. Mei and J. Ouyang, *Macromolecules*, 2008, **41**, 5971–5973.
- 54 S.-S. Yoon and D.-Y. Khang, *J. Phys. Chem. C*, 2016, **120**, 29525–29532.
- 55 D. C. Sun and D. S. Sun, *Mater. Chem. Phys.*, 2009, **118**, 288–292.
- 56 S. Maruthamuthu, J. Chandrasekaran, D. Manoharan, S. N. Karthick and H. J. Kim, *J. Appl. Polym. Sci.*, 2016, **133**, 43772.
- 57 D. Lensen, D. M. Vriezema and J. C. M. van Hest, *Macromol. Biosci.*, 2008, **8**, 991–1005.
- 58 S. Arunsawad, K. Srikulkit and S. Limpanart, *J. Met., Mater. Miner.*, 2014, **24**, 29–34.
- 59 B.-J. Kim, S.-G. Oh, M.-G. Han and S.-S. Im, *Synth. Met.*, 2000, **122**, 297–304.
- 60 H. Zhang and P. L. Dubin, *J. Colloid Interface Sci.*, 1996, **186**, 264–270.
- 61 E. Eren, G. Celik, A. Uygun, J. Tabačiarová and M. Omastová, *Synth. Met.*, 2012, **162**, 1451–1458.
- 62 D. Wang, S. Karato and Z. Jiang, *Geophys. Res. Lett.*, 2013, **40**, 2028–2032.
- 63 T. Tungkavet, N. Seetapan, D. Pattavarakorn and A. Sirivat, *Mater. Sci. Eng., C*, 2014, **46**, 281–289.
- 64 Z. Qi and P. G. Pickup, *Chem. Commun.*, 1998, 2299–2300.
- 65 T. Dai, X. Jiang, S. Hua, X. Wang and Y. Lu, *Chem. Commun.*, 2008, 4279–4281.

